MNRAS **441,** 1444–1456 (2014) doi:10.1093/mnras/stu579

On the relation between specific star formation rate and metallicity

A. Pipino,★ S. J. Lilly and C. M. Carollo

Institute for Astronomy, ETH Zurich, Wolfgang-Pauli-Strasse 27, CH-8093 Zurich, Switzerland

Accepted 2014 March 20. Received 2014 March 18; in original form 2014 January 10

ABSTRACT

In this paper, we present an exact general analytic expression $Z(\mathrm{sSFR}) = \frac{y_Z}{\Lambda(\mathrm{sSFR})} + I(\mathrm{sSFR})$ linking the gas metallicity Z to the specific star formation rate (sSFR), which validates and extends the approximate relation put forward by Lilly et al. (L13), where y_z is the yield per stellar generation, $\Lambda(\mathrm{sSFR})$ is the instantaneous ratio between inflow and star formation rate expressed as a function of the sSFR and I is the integral of the past enrichment history, respectively. We then demonstrate that the instantaneous metallicity of a self-regulating system, such that its sSFR decreases with decreasing redshift, can be well approximated by the first term on the right-hand side in the above formula, which provides an upper bound to the metallicity. The metallicity is well approximated also by $Z^{\mathrm{id}}_{\mathrm{L13}} = Z(\mathrm{sSFR}) = \frac{y_Z}{1+\eta+\mathrm{sSFR}/\nu}$ (L13 ideal regulator case), which provides a lower bound to the actual metallicity. We compare these approximate analytic formulae to numerical results and infer a discrepancy <0.1 dex in a range of metallicities ($\log(Z/Z_\odot) \in [-1.5, 0]$, for $y_z \equiv Z_\odot = 0.02$) and almost three orders of magnitude in the sSFR. We explore the consequences of the L13 model on the mass-weighted metallicity in the stellar component of the galaxies. We find that the stellar average metallicity lags ∼0.1–0.2 dex behind the gas-phase–metallicity relation, in agreement with the data.

Key words: ISM: abundances – galaxies: abundances – galaxies: evolution – galaxies: formation – galaxies: high-redshift.

1 INTRODUCTION

The evolution of the metallicity in galaxies constrains the history of the gas accretion relative to the star formation, as well as the relative importance of outflows. As such, it has been extensively studied at different cosmic epochs. Whilst the full stellar metallicity distribution (SMD) is available only for a few selected nearby galaxies, including the Milky Way and its components, average metallicities in the stars and in the gas of star-forming regions are available for many more objects at different cosmic epochs (O'Connell 1976; Lequeux et al. 1979; Tremonti et al. 2004; Maier et al. 2005, 2006; Savaglio et al. 2005; Erb et al. 2006a,b; Gallazzi et al. 2006; Cid Fernandes et al. 2007; Maiolino et al. 2008; Panter et al. 2008; Mannucci et al. 2009; Sommariva et al. 2012; Zahid et al. 2012; Leja et al. 2013, and references therein). These observations have established that, at any redshift $z < 4$, the most massive galaxies are the most metal rich in both their gas and stellar components. Moreover, at fixed mass, the gas metallicity of star-forming objects decreases with increasing redshift (Erb et al. 2006a,b; Maiolino et al. 2008; Mannucci et al. 2009; Mannucci, Salvaterra & Campisi 2011; Richard et al. 2011; Yuan, Kewley & Richard 2013).

Among the many theoretical attempts to understand the drivers of such relations, analytical chemical evolution models appeal either to a decreasing importance of outflows (e.g. Garnett 2002; Tremonti et al. 2004; Spitoni et al. 2010, and/or differential winds[1], e.g. Dalcanton 2007; Recchi et al. 2008) or to an increase in the star formation efficiency (Dalcanton 2007; Spitoni et all. 2010; Peeples & Shankar 2011), a variation in the yield [via a flattening of the initial mass function (IMF); e.g. Köppen, Weidner & Kroupa 2007] or an increase in the fraction of re-accreted metals (Davé, Finlator & Oppenheimer 2012), with galactic mass, as possible explanations. It is worth pointing out that, in many cases, these models are adopted to interpret the data at a single epoch. On the other hand, galaxy formation numerical experiments, such as cosmological simulations and semi-analytical models, despite qualitatively matching the $z \sim 0$ relation, do not reproduce its slope (e.g. Pipino et al. 2009) and generally suffer from overpredicting the metallicity of high-redshift star-forming galaxies (see, e.g., the discussion in Maiolino et al. 2008, and references therein; Sakstein et al. 2011; Yates et al. 2012).

More recently, a new dimension was added to the observational picture, with studies suggesting that, *globally*, the gas metallicity Z

★ E-mail: axp@astro.ox.ac.uk

[1] Namely the outflows in which the ejection of some chemical species is enhanced with respect to others.

of $z \sim 0$ galaxies depends also on the (specific) star formation rate (SFR): at a fixed galaxy mass, higher metallicities correspond to a lower star formation activity (e.g. Ellison et al. 2008; Mannucci et al. 2010, but see e.g. Yates et al. 2012). Furthermore, there is empirical evidence suggesting the *local* nature of such mass–SFR–Z relation (Rosales-Ortega et al. 2012), and the question becomes as to whether the $Z = Z(M, \mathrm{SFR})$ relation is redshift independent; that is, if high-redshift galaxies populate the extrapolation of the so-called $z \sim 0$ fundamental metallicity relation, that can either be a surface in the mass–SFR–metallicity space (Mannucci et al. 2010) or a plane (Lara-López et al. 2010, 2013) out to $z \sim 2$, or even $z = 3$ (when accounting for changes in the ionization parameter; Cullen et al. 2014; Nakajima & Ouchi 2013). Such a debate is lively and far from being set (see e.g. Richard et al. 2011; Christensen et al. 2012; Cresci et al. 2012; Niino 2012; Wuyts et al. 2012; Belli et al. 2013; Henry et al. 2013; Stott et al. 2013; Zahid et al. 2013; Troncoso et al. 2014). However, irrespective of the final answer, it highlights the importance of fully and simultaneously addressing galaxy evolution in terms of mass–metallicity and mass–SFR relations and their evolution with redshift. It offers an independent test-bed to the above-mentioned analytic chemical evolution models and provides new constraints to the increasing body of theoretical works (e.g. Bouché et al. 2010; Dutton, van den Bosch & Dekel 2010; Lilly et al. 2013, L13, and references therein) aimed at explaining the existence and the evolution of the SFR–mass relation (e.g. Daddi et al. 2007; Elbaz et al. 2007; Noeske et al. 2007; Pannella et al. 2009; Oliver et al. 2010) and/or the cosmic run of the specific SFR (sSFR) with simple models for the galaxy growth.

In particular, L13 show that the $z < 2$ evolution of the sSFR of galaxies may be controlled by the cosmological infall of gas, through the regulating action of the gas reservoir via a Schmidt (1959) linear star formation law. Such a simple model broadly explains at the same time the cosmic evolution of the sSFR (e.g. González et al. 2010; Stark et al. 2013, and references therein) and the stellar-to-halo mass ratio (e.g. Moster et al. 2010). More importantly, the L13 model has the additional appealing property of offering an explanation both to the evolution of the gas phase metallicity and to its scatter at a given epoch by directly linking it to variations in the sSFR with just one equation. That is, the sSFR both enters as a second parameter in setting the metallicity and gives an explanation to the epoch-invariant fundamental metallicity relation, thereby linking the epoch dependence and the SFR dependence of the mass–metallicity relation.

At a fixed epoch, the slope of the mass–metallicity relation is then given by the variation of both the star formation and outflow efficiencies with stellar mass (see also Calura et al. 2009). In L13, however, the instantaneous gas phase metallicity is replaced with the value derived considering the system in equilibrium (i.e. imposing $\mathrm{d}Z/\mathrm{d}t = 0$) for both an ideal case of regulator (steady state at constant gas fraction) and a case in which the gas fraction is slowly changing.

Other analytic models do not either make explicit the sSFR dependence of metallicity (e.g. Dayal, Ferrara & Dunlop 2013) or, despite their similarity to L13, adopt a different notion of 'steady-state' (e.g. constant gas mass evolution; e.g. Davé et al. 2012), claiming that the temporal variation in the metallicity for a given galaxy is driven by the amount of metals ejected in the surrounding medium and then re-accreted. Also in the case of Davé et al. (2012), approximate values for the metallicity are adopted.

Given the important role of metallicity as a constraint to galaxy formation theories and the progresses in the measurement of Z, SFR and stellar masses at progressively higher redshifts, it is important to derive full analytical expressions that link the metallicity evolution to the sSFR evolution of a single galaxy for generic gas accretion and outflow histories. If correct, the above-mentioned approximated formulae (e.g. Davé et al. 2012; L13) could be then re-derived from such general solutions as special cases and applied in suitable regimes of the galaxy growth.

The aim of this paper is thus to validate and extend the L13 relation between Z and sSFR. To this end, we revisit the L13 equations, link them to analytical models of chemical evolution (Pagel & Patchett 1975; Hartwick 1976; Tinsley 1980; Twarog 1980; Matteucci & Chiosi 1983; Clayton 1988; Edmunds 1990; Köppen & Edmunds 1999; Matteucci 2001; Spitoni et al. 2010) and derive a more general relation in which the metallicity Z is an explicit function of the sSFR for arbitrary gas inflow and outflow histories. We then derive simplified relation for the closed box model, the steady state evolution and the L13 model as special cases of the general solution. Furthermore, we study the range of validity and the goodness of the L13 approximation by comparing these results to a direct numerical integration of the same equations as well as to the predictions of full numerical chemical evolution models, which relax some of the assumptions done to make the problem analytically tractable.

Finally, we test the predictions of the L13 model for the evolution of the mass–stellar metallicity relation with redshift in the specific L13 case and compare it to recent observations (Sommariva et al. 2012).

The L13 model and some of its equations are briefly summarized in Section 2 with the double aim to both set the stage, introducing the relevant physical quantities and symbols, and to link it to the standard equation of analytic chemical evolution model. In Section 3, general relations between gas-phase metallicity and sSFR are presented and their special cases discussed. L13 model predictions regarding the stellar average metallicity and its comparison to data are presented in Section 4. Finally, in Section 5, we summarize and discuss our main conclusions.

2 THE L13 MODEL IN THE FRAMEWORK OF ANALYTIC CHEMICAL EVOLUTION

2.1 The regulation of the baryonic content in L13

L13 suggest that the average galaxy evolution can be broadly explained by very simple physics, as it is determined by the host halo accretion rate and regulated by the SFR ψ, which is directly proportional to the interstellar medium (ISM) mass (the 'gas reservoir') via the star formation efficiency ν (see Table 1), that we will keep constant with time. The model also accounts for the action of SFR-related (e.g. supernova-driven) galactic winds.

Let us define μ as the gas fraction $M_{\rm gas}/M_{\rm tot}$, with $M_{\rm tot} = M_* + M_{\rm gas}$. This implies that the sSFR can be written as (equation 7 in L13)[2]

$$\mathrm{sSFR} = \psi/M_* = \nu\, M_{\rm gas}/M_* = \nu \frac{\mu}{1-\mu}\,. \quad (1)$$

The system accretes gas via inflows, with a given accretion rate $\dot{M}_{\rm acc}$. More specifically, the L13 model assumes that haloes grow according to average prescriptions given by fit to numerical simulations (e.g. equation 3 in L13 and references therein). Baryons are

[2] See the appendix for a more general version when a Schmidt law with exponent $1 + x$ is adopted.

Table 1. Input parameters.

	This paper	L13	Remarks
Baryonic accretion rate	$\dot{M}_{\rm acc}$	Φ	Given by cosmological background
SF efficiency	ν	ϵ	Constant (may vary with galactic mass and/or cosmic time)
Gas-to-total fraction	μ	$\nu_{\rm gas}$	–
Gas-to-star fraction	f	μ	–
Infall rate-to-SFR ratio	Λ	$1/f_{\rm star}$	Varies with time
Outflow rate-to-SFR ratio	η	$\lambda/(1-R)$	May vary with time
Yield per stellar generation	y_z	y	Constant
Metallicity of infalling gas	Z_A	Z_0	Constant
Returned fraction	R	R	Constant

accreted proportionally to the dark matter via the universal baryon fraction. A fraction $f_{\rm gal}$ of the accreted baryons can penetrate into the actively star-forming region and be transformed into stars, as well as possibly ejected by winds.

The simplest (ideal) case of such a regulator has the feature of setting the sSFR equal to the specific baryonic accretion rate $\rm sMIR_B$. L13 (cf. their fig. 3) further show that, for any sudden and instantaneous variation in $\rm sMIR_B$, the sSFR adjusts to a value that coincides with $\rm sMIR_B$ on a time-scale set by the shorter among $1/\nu$ and 1/sSFR. The sSFR tracks the $\rm sMIR_B$ also if this is steadily increasing with time. Only when the variation $\rm dsMIR_B/dt < 0$ and occurs on a time-scale which is faster than $1/\nu$, then the sSFR decrease is slower than the drop in the $\rm sMIR_B$.

Our study will focus on the metallicity–sSFR dependence. Therefore, we do not further discuss the dark matter host halo growth. The cycle of inflow-star formation-outflow that we discuss below pertains to the baryons within the galaxy; therefore, our conclusions do not depend on the chosen $f_{\rm gal}$ either, with the assumption that this value is not affected by, e.g., the galactic SFR or the outflows.

Below, we briefly present the relevant equations of L13's model set-up in a slightly different way in order to link the L13 equation and symbols to the terms that are more common in chemical evolution studies and with the aim of summarizing some of L13's key results to the reader, setting the stage for the present study. To this purpose, in Table 1, we summarize the main physical quantities and the symbols adopted in both this work and in L13.

2.2 Basic equations for the evolution of gas mass and metallicity

As in L13, in this paper, we follow the evolution of a galaxy made of gas, assumed to be in a single phase and well mixed at any time, with initial mass $M_{\rm gas,\,0}$, and stars, whose initial mass is set to zero. The evolution of the system can be studied solving an array of equations representing the conservation of the total, the gas and the metal mass in presence of source terms (infall, outflow and nucleosynthesis).

Before doing it, it is convenient to introduce the variables $\Lambda(t)$ and $\eta(t)$, defined in order for the infall and outflow rate to be cast in terms of the SFR $\psi(t)$. Namely the outflow rate $W(t)$ is defined as (Matteucci & Chiosi 1983)

$$W(t) = \eta(t)(1-R)\psi(t), \tag{2}$$

and it is justified by the observational evidences of ubiquitous winds in star-forming galaxies (e.g. Weiner et al. 2005; Bordoloi et al. 2011, 2013; Newman et al. 2012), with mass loading factors comparable to the SFR. Since the same loading factor, within the uncertainties, is observed at different redshifts in galaxies with different SFRs (cf. Newman et al. 2012, and references therein), for a first-order approximation it is reasonable to assume that $\eta \sim$ const in galaxies with SFR-driven winds. Therefore, in the following, we will present both examples and special cases assuming that η is strictly constant in time. On the other hand, in deriving the full solution $Z = Z(\rm sSFR)$, we will let η arbitrarily vary with either time or sSFR.

The infall rate is given by

$$\dot{M}_{\rm acc} = \Lambda(t)(1-R)\psi(t). \tag{3}$$

The term $\Lambda(t)$ was introduced and set to a constant value by Matteucci & Chiosi (1983), to make the problem tractable analytically. The same time-invariant definition (i.e. equation 3 with $\Lambda =$ const) is adopted in many other papers in the literature. In our approach, instead, the equation above is actually inverted and solved for $\Lambda(t)$, which will provide a way for parametrizing how the SFR *instantaneously* responds to changes in the known accretion rate. Therefore, in this case (and in L13's formulation), $\Lambda(t) \propto \frac{\dot{M}_{\rm acc}}{\psi(t)}$ is a function of time and becomes the instantaneous measure of the ratio between the gas accretion rate (given by the cosmological model) and the SFR.

The returned fraction by stars R is defined by invoking the instantaneous recycling approximation (IRA; Schmidt 1963) as

$$R = \int_{1\,{\rm M}_\odot}^{\infty} (m - m_{\rm R})\phi(m)\,{\rm d}m, \tag{4}$$

where $\phi(m)$ is the IMF and $m_{\rm R}$ is the mass of the stellar remnant. The IMF is assumed constant in time. The yield per stellar generation is then defined as (Tinsley 1980)

$$y_Z = \frac{1}{1-R}\int_{1\,{\rm M}_\odot}^{\infty} m p_{Z,m}\phi(m)\,{\rm d}m, \tag{5}$$

where $p_{Z,\,m}$ is the fraction of newly produced and ejected metals by a star of mass m. Finally, Z_A is the metallicity of the infalling gas.

Under these assumptions and definitions, the equations that regulate the evolution of the system in L13 become exactly those used by analytical models for chemical evolution with inflows and outflows (e.g. Pagel & Patchett 1975; Hartwick 1976; Tinsley 1980; Twarog 1980; Edmunds 1990; Köppen & Edmunds 1999; Matteucci 2001; Spitoni et al. 2010),

$$\begin{cases} \frac{{\rm d}M_{\rm tot}}{{\rm d}t} = (\Lambda(t) - \eta(t))(1-R)\psi(t) \\ \frac{{\rm d}M_{\rm gas}}{{\rm d}t} = (\Lambda(t) - \eta(t) - 1)(1-R)\psi(t) \\ \frac{{\rm d}Z\cdot M_{\rm gas}}{{\rm d}t} = (1-R)\psi(t)[\Lambda(t)Z_A + y_Z - (\eta(t)+1)Z] \end{cases}, \tag{6}$$

with the only difference that, in L13 and in this paper, Λ and η may vary with time, not least as the system increases its mass.

Also, both the star formation law and the accretion rate of the galaxy are specified, whereas in standard analytical chemical evolution models, it is customary to express metallicity variations as a function of μ without any explicit dependence on both SFR and $\dot{M}_{\rm acc}$.

Combining the first two equations in the array (6), L13 (see their equation 12) came to the following link between $\Lambda(t)$ and sSFR:

$$\Lambda(t) = {\rm sSFR}(t)/\nu + \eta(t) + 1 + \frac{1}{(1-R)\nu}\frac{{\rm d}\ln f}{{\rm d}t}\,, \tag{7}$$

where $f = M_{\rm gas}/M_* = {\rm sSFR}/\nu$. Equation (15) that we discuss below is a special case of this general relation.

2.3 The gas metallicity in the L13 approach

Rather than explicitly solving equation (6) also for the metallicity, L13 derive approximate solutions by assuming the system to be in equilibrium. That is, by solving the third equation in the array (6) by imposing ${\rm d}Z/{\rm d}t = 0$. Indeed, L13 derive two slightly different approximations for the metallicity: one that holds in the case of an ideal regulator (i.e. with the gas fraction identically constant in time), and one that holds for the more realistic non-ideal regulator (equations 26 and 29 in L13). In the formalism of this paper, these two approximations become

$$Z^{\rm id}_{\rm L13} \equiv \frac{Z_A + y_z}{{\rm sSFR}/\nu + \eta + 1},$$

$$Z_{\rm L13} \equiv \frac{Z_A + y_z}{{\rm sSFR}/\nu + \eta + 1 + \frac{1}{(1-R)\nu}\frac{{\rm d}\ln f}{{\rm d}t}} = \frac{Z_A + y_z}{\Lambda(t)}\,, \tag{8}$$

respectively. We remind the reader that in L13 $\eta = {\rm const}$. Such simple expressions for the metallicity have non-trivial consequences. In the first place, the variation in the sSFR with cosmic epoch will drive a change in the metallicity of a given 'average' galaxy.

Secondly, at any given time, two galaxies with the same stellar mass may have different metallicities, according to the values of the sSFR, η, ν, f that characterize them. In the framework of this analytical model, such a difference in metallicity is caused by the different 'equilibrium' gas fraction in the two galaxies (or equivalently, their sSFR, if the other terms in the denominator are smaller). That is, a mass–metallicity–SFR relation is naturally predicted by the L13 model. More quantitatively, at a given epoch, two galaxies $i = 1, 2$ with given stellar masses M_i will have the ratio of their metallicities given by (assuming $Z_A = 0$, $\eta = 0$, ideal regulator case)

$$\begin{aligned} Z_{\rm L13,1}/Z_{\rm L13,2} &= \nu_1 M_1/\nu_2 M_2\ ({\rm SFR}_2 + M_2\cdot\nu_2)/({\rm SFR}_1 + M_1\cdot\nu_1) \\ &= M_1/M_2\ {\rm SFR}_2/{\rm SFR}_1\ H({\rm sSFR}_i, \nu_i(M_i))\,, \end{aligned}$$

that is,

$$\log(Z_1/Z_2) = \log(M_1/M_2) - \log({\rm SFR}_1/{\rm SFR}_2) + \log(H)\,.$$

3 THE METALLICITY EVOLUTION

The set of equations presented in array (6) with suitable initial conditions are sufficient to characterize the galaxy evolution in terms of its gas mass, gas fraction and metallicity evolution, by direct integration over time. These solutions can then be transformed into an sSFR dependence via the sSFR–μ (equation 1) and sSFR–Λ (equation 7) relations. This will be the core and novel aspect of this paper. In particular, we will derive two versions of a more general solution of the equations which include among their terms both the L13 approximations ($Z^{\rm id}_{\rm L13}$, $Z_{\rm L13}$). We will then show under which conditions and how quickly the other terms in the solutions become negligible and, thus, L13 approximations become good solutions. In the final part of this section, we will compare the full analytical solution to the approximate L13 solution, and both to numerically derived trends, to test the range of validity and the accuracy.

3.1 General solution: Z as a function of time and sSFR

Let us take a step back and start by recalling the formal general solutions for the gas and the metallicity evolution with the explicit time dependence that can be derived by the same set of three equations (6) if one leaves the accretion rate unspecified and further assumes $\eta = {\rm const}$ (in analogy with previous works and L13):

$$M_{\rm gas} = {\rm e}^{-\nu(1-R)(1+\eta)t} \times \left(M_{\rm gas,0} + \int_0^t {\rm e}^{\nu(1-R)(1+\eta)t'} \dot{M}_{\rm acc}(t')\,{\rm d}t' \right) \tag{9}$$

and

$$\begin{aligned} Z \;=\; & y_z \nu (1-R) {\rm e}^{-\nu(1-R)\int_0^t \Lambda(t'){\rm d}t'} \\ & \times \int_0^t {\rm e}^{\nu(1-R)\int_0^{t'}\Lambda(t''){\rm d}t''} \left(1 + \frac{\Lambda(t')Z_A(t')}{y_z}\right) {\rm d}t' \end{aligned} \tag{10}$$

(see also Recchi et al. 2008, for the solution with $Z_A = 0$). For simplicity, we assumed that $Z(0) = 0$ and that ν and η are constant with time. We also assumed no variations in the IMF (and hence in the yield y_z) with either time or mass. These formulae can be obtained as standard solutions of the differential equations of the array (6) in a manner that is similar to what we show in Section 3.3 (equation 19 onwards); therefore, we do not repeat the derivation here.

Assuming that $Z_A = {\rm const}$, substituting $\Lambda(t)$ in equation (10) with the expression given by equation (7) and integrating the resulting expression by parts, it follows that

$$\begin{aligned} Z \;=\; & Z_A + y_z \nu (1-R) \left(\frac{1}{\nu(1-R)(1+\eta+{\rm sSFR}/\nu)} \right. \\ & - \frac{{\rm e}^{-\nu(1-R)((1+\eta)t + \int_0^t {\rm sSFR}(t')/\nu {\rm d}t')}}{\nu(1-R)(1+\eta+{\rm sSFR}(0)/\nu)} {\rm sSFR}(0)/\nu \\ & - \frac{(1+\eta)\,{\rm e}^{-\nu(1-R)((1+\eta)t + \int_0^t {\rm sSFR}(t')/\nu {\rm d}t')}}{{\rm sSFR}/\nu} \\ & \left. \times \int_0^t \frac{{\rm e}^{\nu(1-{\rm R})((1+\eta)t' + \int_0^{t'}({\rm t}'')/\nu {\rm dt}'')}}{\nu(1-{\rm R})(1+\eta+{\rm sSFR}/\nu)^2} \frac{{\rm dsSFR}/\nu}{{\rm dt}'} {\rm d}t' \right) \\ =: & \ (I_1 - I_2 - I_3)\,, \end{aligned}$$

where

$$I_1 \equiv Z^{\rm id}_{\rm L13} = \frac{Z_A + y_z}{1 + \eta + {\rm sSFR}/\nu}\,. \tag{11}$$

Despite two terms in the addition (I_2, I_3 – which incorporate the integral of the accretion history), have still the explicit dependence on time, we made an important step forward as we have the first term ($Z^{\rm id}_{\rm L13}$) depending only on the sSFR. As we will see below, $Z^{\rm id}_{\rm L13}$ is also a bounding value to the true metallicity. To understand the meaning of $I_1 = Z^{\rm id}_{\rm L13}$ in this context, we need to look first at the following special case of the general solution: the evolution at constant gas fraction.

3.2 Special case I – evolution at constant gas fraction

If the galaxy is constantly in an accretion-dominated regime, that is, if we add the assumption that Λ, η are both constant with time and that $\Lambda - \eta > 1$, then $M_{\rm tot}$ increases with time. The gas fraction evolves as (e.g. equation 9 in Recchi et al. 2008)

$$\mu = \mu_{\rm steady} + \frac{f_M}{\Lambda - \eta}\,, \tag{12}$$

where

$$\mu_{\rm steady} = \frac{\Lambda - \eta - 1}{\Lambda - \eta} \tag{13}$$

and

$$f_M = M_{\rm gas,0}/M_{\rm tot}(t)\,. \tag{14}$$

Therefore, the gas fraction tends to the value given by $\mu_{\rm steady}$. This is what we refer to as *steady state*, namely an evolution at a constant gas fraction, whose value is set by the constant $\Lambda - \eta$. In this particular case, it is trivial to combine equations (1) and (13) to show that the sSFR can be expressed as

$$\mathrm{sSFR}/\nu = \Lambda - \eta - 1\,. \tag{15}$$

We note that the convergence towards the asymptotic values is faster for larger ν (the shorter the star formation time-scale) and/or larger Λ.

When the steady state is attained, with Λ, η and the sSFR constant in time, the solution for the metallicity becomes much simpler

$$\begin{aligned} Z_{\rm ss}^{\rm true} &= Z_A + \frac{y_z}{\Lambda}\left(1 - \mathrm{e}^{-\nu(1-R)\Lambda t}\right) \\ &\rightarrow Z_A + \frac{y_z}{\Lambda} = Z_A + \frac{y_z}{1 + \eta + \mathrm{sSFR}/\nu} \end{aligned} \tag{16}$$

at times $t > 1/\nu > 1/(\nu(1-R)\Lambda)$.

That is, the metallicity settles to the constant value given by $Z_{\rm L13}^{\rm id}$. As such, the asymptotic regime for the equilibrium metallicity (i.e. when $\mathrm{d}Z/\mathrm{d}t = 0$) is used in L13 as the value for the metallicity in the case of the ideal regulator (i.e. when the gas fraction stays constant). This result further clarifies the meaning to the $Z_{\rm L13}^{\rm id}$ term (equation 11) contributing to the metallicity in the general equation. It is in fact a 'steady-state-like' term, determined by the current value of the sSFR.

We also derive another interesting result, probably overlooked in the recent literature on the sSFR evolution at high redshift. In particular, equation (15) implies that one can easily model a galaxy evolving at constant sSFR as the result of an accretion-dominated regime where $\Lambda - \eta - 1 = \mathrm{const} > 1$. The results shown in this section imply that, at the same time, the metallicity would not evolve (assuming $Z_A = \mathrm{const}$). Since Z is observed to decrease at $z > 2$, this is another reason to suspect that the sSFR is also not constant at $z > 2$ (see, e.g., Stark et al. 2012).

3.3 Integrating the metallicity equation over the sSFR

One can alternatively set up the differential equation for the metallicity variation as a function of the sSFR as the time variable. With the aim to derive a very general solution, from this section onwards, not only we keep considering Λ as a function of time (and sSFR), but also we relax the assumption of $\eta = \mathrm{const}$ with both time and sSFR. In particular, we note that equation (7) can be rewritten as

$$\frac{\mathrm{dsSFR}}{\mathrm{d}t} = \nu(1-R)\mathrm{sSFR}(\Lambda(t) - \eta(t) - 1 - \mathrm{sSFR}/\nu)\,. \tag{17}$$

Combining the third equation with the second one in the array (6), one can write

$$\frac{\mathrm{d}Z}{\mathrm{d}t} = (1-R)\nu[\Lambda(t)Z_A + y_Z - \Lambda(t)Z]\,. \tag{18}$$

Dividing equation (18) by equation (17), one can derive an expression for $\mathrm{d}Z/\mathrm{dsSFR}$. Some algebra then leads us to the following differential equation for the metallicity:

$$\frac{\mathrm{d}Z}{\mathrm{dsSFR}} + F(\mathrm{sSFR})Z = y_z G(\mathrm{sSFR})\,, \tag{19}$$

where

$$G(\mathrm{sSFR}) = \frac{1 + \frac{Z_A\Lambda}{y_z}}{\mathrm{sSFR}/\nu(\Lambda - \eta - 1 - \mathrm{sSFR}/\nu)} \tag{20}$$

and

$$F(\mathrm{sSFR}) = \frac{1}{\frac{1}{\Lambda} + \frac{Z_A}{y_z}}\,G(\mathrm{sSFR})\,. \tag{21}$$

This equation has the following formal solution:

$$Z = y_z \mathrm{e}^{-\int_{x_0}^{x} F(x')\,\mathrm{d}x'} \int_{x_0}^{x} \mathrm{e}^{\int_{x_0}^{x'} F(x'')\,\mathrm{d}x''} G(x')\,\mathrm{d}x'\,, \tag{22}$$

where $x = \mathrm{sSFR}/\nu$. Integrating by parts, with the further assumption that $Z_A = \mathrm{const}$, the solution can be written as

$$Z = Z_A + \frac{y_z}{\Lambda(x)} - y_z \mathrm{e}^{-\int_{x_0}^{x} F(x')\mathrm{d}x'} \int_{x_0}^{x} \frac{\mathrm{e}^{\int_{x_0}^{x''} F(x')\mathrm{d}x'}}{\Lambda(x'')^2}\,\frac{\mathrm{d}\Lambda}{\mathrm{d}x''}\mathrm{d}x''\,. \tag{23}$$

This new way to solve for the metallicity uses the sSFR itself as the time variable. This formal analytic solution is similar to equation (11)[3], with the difference that here we make explicit the contribution by the instantaneous value of $\Lambda(t)$ and $\eta(t)$ as if it were in the steady state, that is,

$$\begin{aligned} Z_{\rm ss}^{\rm inst} &= Z_A + \frac{y_z}{\Lambda} = Z_A + \frac{y_z}{\mathrm{sSFR}/\nu + \eta + 1 + \frac{1}{(1-R)\nu}\frac{\mathrm{d}\ln f}{\mathrm{d}t}} \\ &\equiv Z_{\rm L13}\,, \end{aligned} \tag{24}$$

namely the value of the metallicity adopted in L13 for the 'non-ideal regulator' (i.e. gas fraction slowly varying in time). The other term in the addition is the 'resistance' to move to the new steady state, $-\tilde{I}_2$, given by the past chemical evolution history. With this version of the general solution for the metallicity, we made explicit the fact that $Z_{\rm L13}$ is one of the terms that contribute to the actual metallicity of the galaxy in the general case. Equation (23) readily tells us that, when $\tilde{I}_2$ is small (as in the L13 model), the evolution of galaxies can be approximated by a sequence of steady state solutions with lower equilibrium gas fractions (lower sSFR) and higher metallicities. We quantify this statement in the next section.

3.4 Special case II – accretion rate slowly changing with time (L13)

Having derived general formulae linking the metallicity to the sSFR for arbitrary gas accretion histories (equations 11 and 23), we can now discuss the L13 approximations. In order to move from the general equations discussed above to the L13 special cases, we simply need to add the assumption – explicitly made in L13 – that the sSFR slowly changes in time in order to better quantify the other terms ($I_2, I_3, \tilde{I}_2$) in both equations (11) and (23). In particular,

[3] The formal derivations of the solutions are exactly the same.

we now discuss the case in which the sSFR slowly decreases following the cosmological decrease in $\mathrm{sMIR_B}$. As a matter of fact, similar considerations can be done for a slowly increasing sSFR, driven by, e.g., an increasing accretion rate; therefore, we do not further discuss this specific case and refer the reader to L13 (cf. their fig. 3) for some examples on how quickly the sSFR responds to changes in either direction in the accretion rate. For simplicity, we also assume that $Z_A = 0$, since it only adds a constant offset.

For a smoothly declining accretion history, it follows that

(1) as discussed in L13 (their equation 39), $\frac{\mathrm{dln}f}{\mathrm{d}t}$ is small, but finite and negative, hence

$$\frac{1}{\mathrm{sSFR}/\nu + \eta + 1 + \frac{1}{(1-R)\nu}\frac{\mathrm{dlnf}}{\mathrm{dt}}} > \frac{1}{\mathrm{sSFR}/\nu + \eta + 1}. \quad (25)$$

Therefore, $Z^{\mathrm{id}}_{\mathrm{L13}} < Z_{\mathrm{L13}}$. Moreover

(2) $\tilde{I}_2 > 0$. Therefore, $Z < Z_{\mathrm{L13}}$.

(3) Also, I_2 falls off exponentially. Therefore, $I_2 \simeq 0$, for practical purposes, whereas $-I_3 > 0$, as the time derivative of the sSFR is negative. Therefore, $Z > Z^{\mathrm{id}}_{\mathrm{L13}}$.

By combining these results together, we derive that the true value of the metallicity is always within the range $[Z^{\mathrm{id}}_{\mathrm{L13}}, Z_{\mathrm{L13}}]$. This shows that, for a large class of models with the sSFR slowly decreasing in time, rather simple expressions (equations 11–24) can be used to bracket the actual gas-phase metallicity. In other words, for $\dot{M}_{\mathrm{acc}}$ decreasing with time, the true metallicity will be bound between $Z^{\mathrm{id}}_{\mathrm{L13}}$ (the steady-state-like metallicity set by the current value of the sSFR, the ideal regulator case in L13) and Z_{L13} (the steady-state metallicity set by the current value of $\Lambda(t)$, in L13 this is the formula used when the gas fraction is allowed to vary in the non-ideal regulator case).

The next step is to assess the goodness of the approximation of using the steady-state(-like) metallicities (i.e. either $Z^{\mathrm{id}}_{\mathrm{L13}}$ or Z_{L13}) as an estimate of the current metallicity for these systems. This will be the topic of the next section. Here, we conclude by highlighting the qualitative explanation. In the chemical evolution literature terms, the L13 smoothly evolving model is equivalent to a system in which the metallicity varies in response to a slowly changing $\Lambda(t)$. Among others, the behaviour of Z in the varying $\Lambda(t)$ case, has been also graphically and qualitatively discussed by Köppen & Edmunds (1999). When, e.g., $\Lambda(t)$ slowly decreases with time, the system evolves along the locus of the steady-state solutions on the $\mu-$Z plane, moving towards lower gas fractions and higher metallicities. That is, from the steady state set by $\Lambda(t - \mathrm{d}t)$ and $\eta(t - \mathrm{d}t)$ to a new steady state [given by the current value of $\Lambda(t)$ and $\eta(t)$], where the new μ_{steady} is lower than the old one, whereas Z_{steady} increases (Köppen & Edmunds 1999, their figs 5 and 6).

3.4.1 The accuracy of the L13 approximation: comparison to full analytic solutions

If one further adopts the initial condition $\mu = 1$ (no stars), then $x_0 = \mathrm{sSFR}(0)/\nu$ diverges. Therefore, we can assume $x_0 = \infty$ in equation (23).

In L13, the sSFR decreases with time, driven by a decrease in $\dot{M}_{\mathrm{acc}}$. The variation is slow and at late times $|\frac{\mathrm{dsSFR}}{\mathrm{d}t}|/\mathrm{sSFR} \ll 1$; this implies also a very small variation in the gas fraction (μ or equivalently f). Therefore, there exists an epoch t_1 where $\mathrm{sSFR}/\nu = x_1 \ll 1 + \eta$ and $\Lambda \simeq 1 + \eta$. This implies that $\frac{d\Lambda}{\mathrm{d}x} \to 0$ when $t > t_1$ ($x < x_1$).

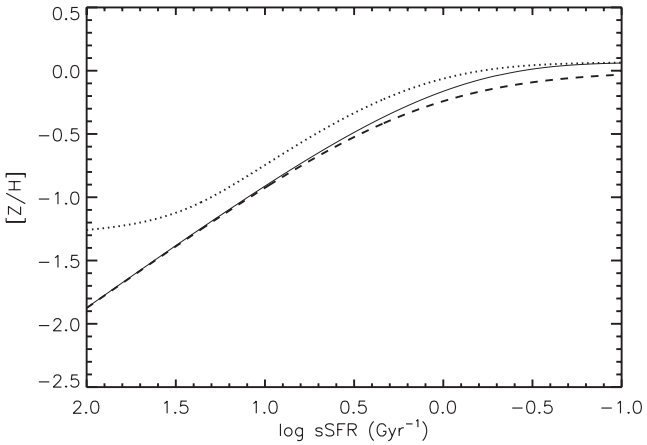

Figure 1. Evolution of the metallicity as a function of the sSFR for galaxies evolving according to the L13 model. The solid line is the evolution given by the numerical integration of equation (10), whereas the dashed line is the metallicity approximated as $Z \sim Z^{\mathrm{id}}_{\mathrm{L13}}$ (equation 11, see text). Finally, the dotted line gives the metallicity approximated by Z_{L13} (equation 23).

As a consequence, we can write

$$\tilde{I}_2 = \int_{x_0}^{x} \frac{\mathrm{e}^{\int_\infty^b F(a)\mathrm{d}a}}{\Lambda(b)^2}\frac{\mathrm{d}\Lambda}{\mathrm{d}b}\mathrm{d}b \simeq \int_{\infty}^{x_1} \frac{\mathrm{e}^{\int_\infty^b F(a)\,\mathrm{d}a}}{\Lambda(b)^2}\frac{\mathrm{d}\Lambda}{\mathrm{d}b}\mathrm{d}b\,,$$

that is, $\tilde{I}_2$ is effectively constant at $x < x_1$ (i.e. at late times).

At the same time, the exponent of the factor in front of $\tilde{I}_2$ grows in absolute value; therefore, the second term in equation (23) is

$$\mathrm{e}^{-\mathrm{const}/x} \times \tilde{I}_2 \to 0.$$

In this case, equation (23) trivially reduces to

$$Z \simeq \frac{y_z}{\Lambda(x)} \equiv Z_{\mathrm{L13}}\,. \quad (26)$$

Similarly, I_3 is small because it has an exponentially declining factor and in the integral we have $|\frac{\mathrm{dsSFR}/\nu}{\mathrm{d}t'}| \ll (1 + \eta + \mathrm{sSFR}/\nu)^2$. We already discussed that I_2 has a fast exponential decline. Therefore, also the 'corrections' given by I_2 and I_3 to the metallicity in equation (11) are small.

To reinforce our findings, in Fig. 1, we compare the numerical integration of the metallicity (solid line) with these two limiting values (dashed – $Z^{\mathrm{id}}_{\mathrm{L13}}$, lower limit; dotted – Z_{L13}, upper limit) for a particular set of ν, y_z and given gas accretion history. For the sake of simplicity, we also arbitrarily set $y_z = 0.02 = \mathrm{Z}_\odot$, $\eta = 0$ and $\nu = 1\ \mathrm{Gyr}^{-1}$.

The formula $Z = Z^{\mathrm{id}}_{\mathrm{L13}} = \frac{y_z}{1+\eta+\mathrm{sSFR}/\nu}$, used by L13 for the ideal regulator case (and $Z_A = 0$) gives always an excellent approximation, departing from the numerical solution only by 0.1 dex at very late stages. It is the best approximation of the true metallicity at the highest values of the sSFR.

On the other hand, the difference $Z - Z_{\mathrm{L13}}$ is significant in the very early phases of the evolution, when $\Lambda(t)$ and sSFR are uncorrelated. This is however a consequence of our set-up. In fact, assigning an initial $\mu = 1$ leads the model to evolve by consuming the gas mass initially present in a way that is independent from the inflow, as a closed box. A different initial set-up might reduce the difference between Z_{L13} and the actual metallicity in these early phases. At late times, instead, in this example, Z_{L13} gives a very accurate approximation of the true metallicity.

3.5 Special case III – the closed box model in terms of the sSFR

Before comparing the analytic approximate solutions to other numerical models, we mention that, in the case of a model with neither accretion nor outflows ($\Lambda = \eta = 0$, closed box approximation, also known as the simple model), the relation between metallicity and sSFR trivially is

$$Z = y_z \ln \frac{1 + \mathrm{sSFR}/\nu}{\mathrm{sSFR}/\nu} \tag{27}$$

which, at early times (high sSFR), has the following approximate behaviour:

$$Z \simeq y_z \nu/\mathrm{sSFR} \simeq y_z \nu/(1 + \mathrm{sSFR}) \tag{28}$$

which is very similar to $Z^{\mathrm{id}}_{\mathrm{L13}}$ when $Z_A = \eta = 0$. As the closed box model well approximates the behaviour of a model with $\Lambda(t) \neq 0$ at early times (high gas fraction; e.g. Köppen & Edmunds 1999), this last equation is a good representation of the general equation behaviour in the regime of high sSFRs.

Therefore, we can conclude that the sSFR, rather than Λ, seems to be the key quantity to accurately estimate the gas metallicity of the system in a variety of cases. The reasons lies in its close relation to the gas fraction μ.

Also, in the closed box model, the star formation has an exponential decline with time-scale $\tau = \nu(1 - R)$. The results in this section then provide a ready estimate for a self-consistent evolution of the metallicity and sSFR for the widely adopted exponentially decaying star formation histories.

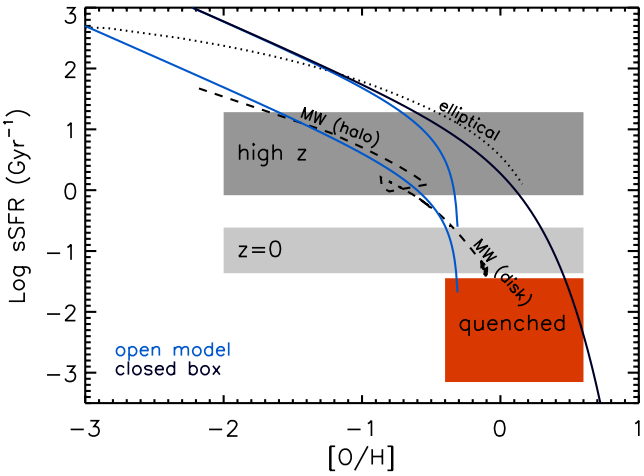

Figure 2. Evolution of the metallicity as a function of the sSFR. The dashed line is the evolution predicted by a full numerical chemical evolution model tuned to reproduce the Milky Way (MW) properties, whereas the dotted line is the prediction for a model calibrated on both local ellipticals (Pipino & Matteucci 2004) and high-redshift galaxies (Pipino et al. 2011). The solid lines give the metallicity approximated as $Z \sim Z^{\mathrm{id}}_{\mathrm{L13}}$ (see text) for models with accretion (blue) and closed box (black). In this illustration, $Z_A = \eta = 0$, $y_z = 0.01$ and ν are matched to that used in the full numerical chemical evolution models. Dark (light) grey areas give the typical values of the sSFR observed in high-(low-)redshift galaxies, whereas the red box highlights the sSFR values for quenched systems.

3.6 The accuracy of the L13 approximation: comparison to full chemical evolution models

The IRA is not a good approximation to follow a system for a long (>1 Gyr) time, even if we focus on the total metallicity, which is dominated by O (produced on a short time-scale) and/or on metallicity inferred from O lines (among others). That is, when $\mu \ll 1$ and after several Gyr of evolution, the effects of metals being recycled by low-mass stars cannot be ignored. We therefore further tested equation (11) against the predictions of full numerical chemical evolution models calibrated on the abundance pattern of the Milky Way and the properties of local ellipticals. We refer the reader to Pipino & Matteucci (2004), Pipino et al. (2011) and Calura et al. (2009) for a description of these models, and to Pipino, Calura & Matteucci (2013) for their predicted sSFRs. The comparison is shown in Fig. 2, where the tracks in the metallicity–sSFR plane are shown for both analytical (solid) and numerical [dashed, Milky Way (MW); dotted, elliptical] models. In the analytical models, ν is matched to that used in the full numerical chemical evolution simulations. For the same reason, we set $\eta = Z_A = 0$. The $Z \sim Z^{\mathrm{id}}_{\mathrm{L13}}$ approximation works well for a wide range in sSFR, becoming less accurate at late times for the case of the Milky Way as expected. The difference is however less than a factor of 2, comparable to the observational uncertainty in deriving the gas-phase metallicity. As far as elliptical galaxies are concerned, we note that the closed box approximation (solid black line) works better than the case with an infall with a long time-scale (solid blue lines). This is not unexpected since these galaxies should have formed on a short time-scale (e.g. Matteucci 1994), or equivalently, at high sSFR (e.g. Pipino et al. 2013, and references therein). In the numerical models, the galactic wind prevents the star formation to occur at arbitrarily low gas fractions (hence sSFR), whereas the ideal closed box systems proceeds with $\mu \to 0$. To guide the eyes, dark (light) grey areas give the typical values of the sSFR observed in high-(low-)redshift galaxies, whereas the red box highlights the sSFR values for quenched systems at $z \sim 0$.

From this comparison, we can therefore conclude that a quasi-steady-state evolution depicted in analytic models (as in L13) must be typical of relatively low sSFR, disc galaxies, possibly representing the majority of the star-forming 'main sequence' at $z < 2$. For these galaxies, the current metallicity is well approximated by a steady-state-like value set by the current sSFR. We suggest here that ellipticals, instead, evolve at higher sSFR for a given metallicity than spiral galaxies for a given mass, in a suggestive analogy to what happens in the [α/Fe]–[Fe/H] plane (e.g. fig. 4 in Matteucci & Brocato 1990). That is, highly α-enhanced stellar populations are a distinctive feature of galaxies formed with high average sSFR, similar to those observed at $z > 2$ (cf. Pipino et al. 2013, see also discussions in Peng et al. 2010, in the context of empirical models of galaxy growth, and in Pipino et al. 2009 – their section 3.2 – in the context of semi-analytical models of galaxy formation). Clearly, having adopted the IRA to make the problem analytically tractable, any abundance ratio predicted in the framework of this paper (and in L13) will be constant in time and simply equal to the ratio of the yields, unless one invokes selective inflows/outflows. Therefore, we cannot predict an analytical quantitative relation between sSFR and α/Fe ratio in the gas of a star-forming galaxy.

We stress, however, that the 'morphology' classes introduced in this section simply refer to the two typical parametrizations adopted in numerical chemical evolution simulations. Namely high ν and quick infall are needed to reproduce the chemical abundance pattern of present-day ellipticals, whereas smaller ν and longer accretion histories seem to be typical of spirals. Therefore, in the context of this paper, such 'morphological' classes should be understood as useful terms for linking the L13 model (and the more general equations presented in this paper) to special cases of standard numerical models of chemical evolution. A link between the actual

morphology of the galaxies and the L13 model is beyond the scope of this paper.

Finally, one can exploit Fig. 2 as a diagnostic plot to readily estimate the star formation efficiency of a given galaxy observed at a given epoch, by simply comparing its location in the sSFR–metallicity plane with a set of model predictions at fixed yield (IMF) and varying ν.

As mentioned above, the IRA does not hold at time-scales comparable with those of massive stars. This would have a noticeable effect if we were dealing with the chemical abundance ratios produced by a single stellar generation. On the other hand, it is important to note that the metal return of a stellar generation does not depend on the infall/outflow history.

In the earliest phases of the galaxy evolution, when the systems are not smoothly evolving, the biggest uncertainty in the derivation of the actual gas metallicity Z is not related to the computation of the yield per se (and hence the assumption of the IRA), but probably comes from the assumption of the ISM being always homogeneous and well mixed, as there might not be enough time for the metals to, e.g., cool down in new star-forming sites or to travel a long distance. Equation (24) will still hold on a suitably chosen local level, if one replaces the infall metallicity Z_A with that inflowing from neighbouring regions, and considers that the wind term will pollute the ISM immediately around the star-forming region. On a galaxy-wide scale, a suitable convolution of such a local version applied to all star-forming regions would then give the overall metallicity evolution.

4 THE METALLICITY IN THE STARS OF L13 GALAXIES

4.1 The SMD

Let us start by showing the expected SMD in the framework of the L13 model, that is, the fraction of stars per metallicity bin. In order to illustrate the SMDs behaviour, we show in Fig. 3 a sample of galaxies smoothly evolving according to L13. In this example, the galaxy final masses are in the range $10^{9-11}\,\mathrm{M}_\odot$, and we assume that the more massive the galaxy, the higher the ν (in the range 0.1–1.3 Gyr^{-1}). We also assume that $Z_A = 0$ and a formation redshift, namely when the SFR is switched on, of $z_\mathrm{F} = 10$. From the figure, we can qualitatively infer an increase in the gas phase metallicity

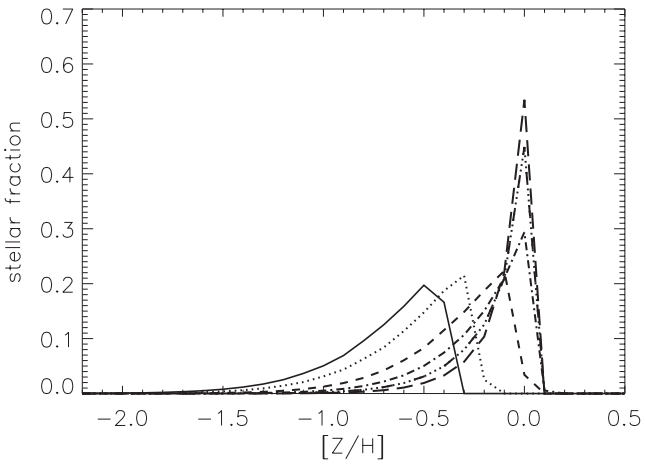

Figure 3. Predicted SMD for arbitrary galaxy models evolving as prescribed by the L13 framework. See text for details.

created by the variation in ν is mirrored by an increase in the average stellar metallicity. In particular, the average metallicity in the most evolved (i.e. most massive) galaxies already attained its uppermost boundary, set by the yield (e.g. Edmunds 1990), $y_z = 0.02$ in this illustration. The larger star formation efficiency at high masses makes the SMD rather sharply peaked around $Z \sim y_z$. Lower mass systems are still building up their SMD, which shows a long low-metallicity tail and a sharp cut-off at Z corresponding to the current gas metallicity.

4.2 Gas versus stellar (average) metallicity

Since the SMD of a galaxy is rarely accessible, it is useful to discuss other diagnostics that involve, e.g., the mass-weighted stellar metallicity, defined as (Pagel & Patchett 1975)

$$Z_* = \frac{1}{M_*}\int_{M_0}^{M_*} Z(M)\,\mathrm{d}M \simeq \frac{y_z}{M_*}\int_{M0}^{M_*}\frac{\mathrm{d}M}{1+\eta+\mathrm{sSFR}/\nu}$$
$$= \frac{y_z\nu(1-R)}{M_*}\int_0^t M(t')\frac{\mathrm{sSFR}(t')/\nu}{1+\eta+\mathrm{sSFR}(t')/\nu}\mathrm{d}t', \qquad (29)$$

where M_* is the total mass of stars ever born contributing to the light at the present time, $Z(M)$ is the metallicity in the gas forming a given stellar generation of mass $\mathrm{d}M$ and we approximated the metallicity with $Z^\mathrm{id}_\mathrm{L13}$. For simplicity's sake, we neglect the metallicity of the infalling gas and assume $\eta = \mathrm{const}$.

Next, we consider that

$$M(t')\mathrm{sSFR}(t')(1-R) = \mathrm{SFR}(t')(1-R) = \frac{\mathrm{d}M}{\mathrm{d}t'}. \qquad (30)$$

We make this substitution in equation (29), and we then integrate the right-hand side by parts further assuming that $M_0 = M(0) \sim 0$ (and hence $\mathrm{sSFR}(0) = \infty$). It follows that

$$Z_* \simeq \frac{y_z}{M_*}\times\left(\frac{M_*}{1+\eta+\mathrm{sSFR}(t)/\nu}\right.$$
$$\left. -\int_0^t M(t')\frac{|\mathrm{dsSFR}/\mathrm{d}t'|}{\nu(1+\eta+\mathrm{sSFR}(t')/\nu)^2}\,\mathrm{d}t'\right), \qquad (31)$$

where we also consider that the sSFR decreases with time. As for the gas metallicity solutions, it is easy to recognize a term in equation (31) that is similar to the L13 steady state/ideal regulator approximation for the current gas metallicity (equation 11 in this paper), and another containing the integral of the past history, whose magnitude is related to the variation of the sSFR with time.

The gas-phase metallicity is an instantaneous measure, which should coincide with the metallicity of the stars in the metal-rich tail of the SMD, namely the most recently formed. The average stellar metallicity also accounts for the earlier (more metal-poor) stellar generations, and hence it will be always lower than the gas phase one, the difference being roughly given by the second term in the right-hand side of equation (31).

Generally, a large difference between gas and average stellar metallicity is found in the closed box model, which features an exponentially decreasing star formation history. Therefore, most of the stars have a very low metallicity (i.e. the classic G-dwarf problem). The most extreme departure, however, is in the final stages, where $Z_\mathrm{gas} \to \infty$ and $Z_* \to y_z$ for $\mu \to 0$. At the opposite end, a steady-state model ($\Lambda - \eta > 1$, with both Λ and η constant in time) has the property that $Z_* = Z_\mathrm{gas}$ when it reaches equilibrium

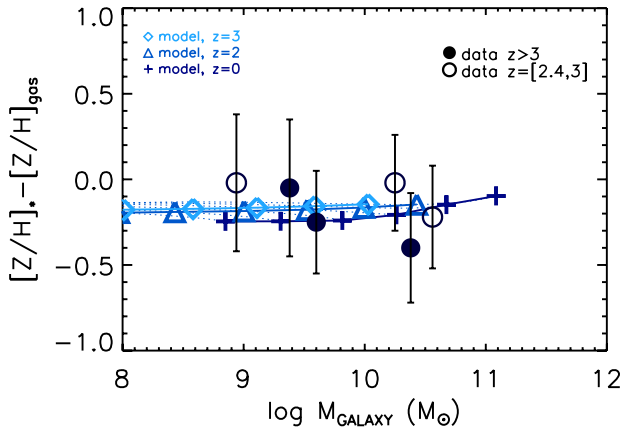

Figure 4. Difference in metallicity between galactic components and its evolution as a function of the stellar mass. Models as in Fig. 3. Crosses, triangles and diamonds give the position on each track at $z = 0$, 2 and 3, respectively. Single galaxy measurements in the redshift bins [2.4–3[(empty circles) and [3,3.7] (full circles), respectively, as compiled by Sommariva et al. (2012) are also shown.

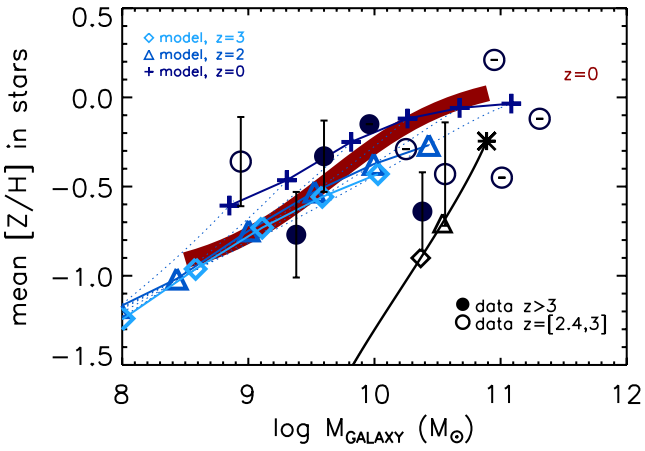

Figure 5. Stellar metallicity evolution as a function of the stellar mass. Models as in Figs 3 and 4. Crosses, triangles and diamonds give the position on each track at $z = 0$, 2 and 3, respectively. The predictions for the closed box model system with $\nu = 0.3$ Gyr^{-1} are shown by the (almost vertical) solid black line. The fit to the local observed relation (Panter et al. 2008, thick solid line) and single galaxy measurements in the redshift bins [2.4–3[(empty circles) and [3,3.7] (full circles), respectively, as compiled by Sommariva et al. (2012) are also shown.

(see also Köppen & Edmunds 1999); therefore, in this case, we have the smallest difference at any time.

Models like the one discussed here (and in L13) have an intermediate behaviour between these two cases. Qualitatively, this can be understood as these models tend to converge to $\Lambda(t) - \eta \simeq 1$ at late times; therefore, both $Z_{\rm gas} \rightarrow y_z$ for small μ and $Z_* \leq y_z$ (e.g. Edmunds 1990), making the difference smaller than in the closed box model case. In earlier phases of the evolution, the SFR is steadily increasing in time, making the SMD strongly skewed towards large Z. Therefore, at these early epochs, the youngest stellar generations (whose composition is the same that of the gas-phase) have a large weight in the computation of the average stellar metallicity. This finding implies that the evolution in the stellar metallicity in the L13 framework can be approximated, for a ready and quick estimate, with a relatively simple dependence on the sSFR, which mirrors that of the gas-phase metallicity (equation 11). Equation (31) implies the existence of a mass–metallicity–SFR relation also in the case of the stellar metallicities, whereby galaxies evolving on tracks at higher sSFR have lower mass-weighted stellar metallicities. In the light of what has been just discussed, this behaviour should be detectable in the earliest phases, whereas it would become less and less evident when the galaxy has passed the peak of its SMD, with Z_* approaching the yield.

More quantitatively, in the L13 model, we have $|{\rm dsSFR}/{\rm d}t|/{\rm sSFR} \simeq 2.2/t$, namely decreasing with time and becoming less than 1 at times larger than ∼2.2 Gyr, that is, roughly below $z = 3$. This means that, for most of the galactic evolution, the stellar metallicity is lower, but close, to the current gas metallicity.

We illustrate this in Fig. 4, where we show again the model galaxies presented in Fig. 3: they feature an average stellar metallicity lagging <0.2 dex behind the gas-phase metallicity at high redshift at any mass, where crosses, triangles and diamonds give the position on each track at $z = 0$, 2 and 3, respectively. The model predictions agree with the data (Halliday et al. 2008; Sommariva et al. 2012), which however feature large associated uncertainties.

4.3 The mass–average stellar metallicity relation

We note that since the average metallicity in gas increases with galactic mass, we expect L13 model to predict also a stellar mass–metallicity relation. We show that it is broadly consistent with observations in Fig. 5, where we plot the evolution in the stellar metallicity as a function of the stellar mass. Crosses, triangles and diamonds give the position on each track at $z = 0$, 2 and 3, respectively. We also show the fit to the local observed relation (Panter et al. 2008, thick maroon line) and single galaxy measurements in the redshift bins [2.4–3[(empty circles) and [3,3.7] (full circles), respectively, as compiled by Sommariva et al. (2012).

From the model-to-data comparison point of view, we highlight that, at $z \sim 0$, the predictions for high-mass galaxies seem to match the observations, whereas there is some tension at the low-mass end. On the theoretical side, the slope can be further steepened by acting on the relation between ν and the initial mass. The normalization of the predicted relation can be further adjusted by acting on the yield and of $z_{\rm F}$. These were however chosen to match both the $z \sim 0$ and the $z \sim 2$ mass–metallicity relation of the gas-phase. On the observational side, a caveat is that $z \sim 0$ data include passive galaxies, which tend to be the most massive and metal-rich galaxies. We can therefore expect a milder observational slope in the mass–stellar metallicity relation, when selecting only star-forming galaxies, in better agreement with our model. The existence of metallicity gradients and aperture effects may further complicate the comparison between data and models. On the other hand, while we predict mass-weighted metallicities, the observables in questions are luminosity-weighted quantities. The difference between luminosity-weighted and mass-weighted metallicity is negligible in massive, old, non-star-forming galaxies (e.g. Arimoto & Yoshii 1987), which make the high-mass end of the local relation in Fig. 5. At smaller masses, the mass-averaged Z are slightly larger than the luminosity-averaged ones, since the latter give more weight to the earliest low-metallicity stellar populations (see e.g. Pipino, Matteucci & Chiappini 2006). This may explain the offset between $z = 0$ predictions and observations at the low-mass end in Fig. 5.

In our models, we do see an evolution in the metallicity with redshift at a given mass at $z < 2$. This is slightly (∼0.1 dex) smaller to that predicted in the gas phase, and shown in L13 (their fig. 7). No apparent evolution is predicted between $z = 2$ and 3. L13

model, however, predicts an evolution of the metallicity in this range, and the variation can be readily estimated as follows: when the nebular emission line correction is included sSFR($z \geq 3$) $\sim$ 6 Gyr^{-1}, whereas sSFR($z = 2$) $\sim$ 2 Gyr^{-1} (e.g. Stark et al. 2013). If we apply equation (11), we would infer an increase in metallicity by a factor of $\sim$2 (0.3 dex) between redshift $z \sim 3$ and $z \geq 2$ matching the observational data (e.g. Maiolino et al. 2008). In the same time-frame, however, given these sSFR, galaxies increase their mass by at least a factor of 2, therefore, they move almost diagonally in the $\log Z_{\rm gas} - \log M_{\rm GALAXY}$ plane. Since in these earlier phases the average stellar metallicity tracks very well the gas metallicity, the model predicts a similar evolution also in the $\log Z_{*} - \log M_{\rm GALAXY}$ plane. The combination of the two effects leads us to an apparent non-evolution in the mass–metallicity plane, as galaxies move along a given track close to the 1:1 relation. They will then move up in metallicity at almost constant mass at $z < 2$, when the sSFR is such that the stellar mass increase is milder than the change in Z.

Sommariva et al. (2012), on the basis of the same data displayed in Fig. 5, seem to favour instead a lack of evolution at all redshifts. It is however important to note the large observational errors and the scatter affecting the $z > 2$ measurements of a few single galaxies.

For comparison, we display the evolution of a galaxy evolving as a closed box model (solid black line) in Fig. 5. We can safely conclude that the data strongly disfavour closed box and favour flow through models like that of L13.

It also useful to remind the danger of comparing mass-weighted predicted quantities to luminosity-weighted observables. This effect is more important at high z, when galaxies feature high SFRs. We stress again that the $z \sim 0$ data mix active and passive galaxies, whereas the high-redshift data points refer to star-forming galaxies. Moreover, while $z \sim 0$ metallicities are mostly related to the optical part of the spectrum, in high redshift galaxies are derived by means of UV absorption lines (Rix et al. 2004). Therefore, a direct and robust, entirely empirical, comparison between the metallicity of the bulk of the stars in galaxies at different redshift has yet to come.

5 DISCUSSION AND CONCLUSIONS

5.1 The gas phase metallicity

5.1.1 On the variation of the Z *as a function of the sSFR evolution*

In this paper, we explored the dependence of gas-phase metallicity on the sSFR. In particular, we derived general analytic formulae that relate the gas phase metallicity to both the infall-to-SFR ratio and the sSFR, for the case of single-zone single-phase galaxies and a linear Schmidt (1959) star formation law. The derived relations take the typical form $Z(\mathrm{sSFR}) = \frac{yz}{\Lambda(\mathrm{sSFR}/\nu)} + I(\mathrm{sSFR}/\nu)$, where I is the integral of the past enrichment history over the sSFR.

In this paper, both the inflow- and the outflow-to-SFR ratios are functions of time (equivalently of the sSFR) and may depend on the input cosmology, the amount of gas that may penetrate the star-forming regions of galaxies and the adopted star formation law. It is important to stress that this approach is different from that adopted in many analytical chemical evolution works in the literature, and still in use to interpret the metallicity of galaxies. These studies adopt Λ and η constant, that is, they do not take into account that realistic outflow- and inflow-to-SFR ratios may change with time as the result of the evolution of the galaxy. Therefore, when they are compared to data at a given redshift, they can only give a simple parametrized understanding of the mass–metallicity relation at that fixed epoch, rather than offering a comprehensive view of galaxy evolution with time.

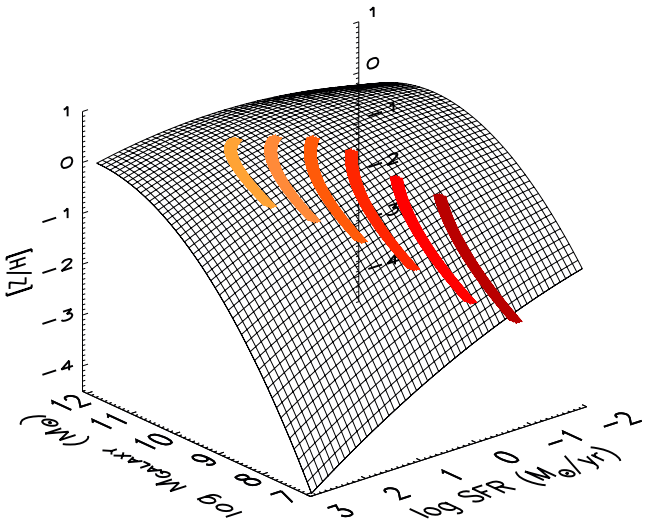

Figure 6. $z < 4$ evolution of the models discussed in Figs 3 and 4 in the three-dimensional space given by SFR, mass and metallicity. The shaded area is the analytical formula of the fundamental metallicity relation given by Mannucci et al. (2010).

We show that in many circumstances (early evolution, quasi-steady-state evolution with slowly decreasing sSFR) a good estimate of the gas-metallicity is obtained by the value $Z^{\rm id}_{\rm L13}$ that the system would have if in steady-state evolution with the infall-to-star formation ratio set by the current value of the sSFR (equation 11), that is, as in the ideal regulator case of L13. On the other hand, a metallicity obtained by current value of the infall-to-SFR, i.e. $Z_{\rm L13}$ (equation 8, L13 non-ideal regulator case), would slightly overestimate the current metallicity of the system. These two values bracket with high accuracy the current metallicity of the system. Therefore, we provide the formal justification to L13 approximations and extend their validity to a larger range of cases. In particular, the formula adopted by L13 for the ideal case is exact for systems with $\Lambda - \eta > 1$ and $\Lambda, \eta = \mathrm{const}$. It is also a good approximation of the actual metallicity for galaxies with slowly decreasing accretion rates.

Also, we add that, since we did not specify anything on both the size and the geometry of what we called the 'galaxy', the equations in principle hold at both the *local* (i.e. for each star-forming region) and the *global* galaxy level, with the latter being a suitable weighted average of the single star-forming regions. Such a theoretical expectation seems to be corroborated by very recent observations (Rosales-Ortega et al. 2012).

Finally, L13 (their fig. 7) show the predictions for the mass–metallicity relation at $z > 0$ in some specific cases calibrated on either the Mannucci et al. (2010) or the Tremonti et al. (2004) $z \sim 0$ relations. A qualitative agreement with the $z \sim 2$ data is achieved. In this paper, we do not repeat the exercise. However, in Fig. 6, we plot the $z < 4$ tracks of the models shown in Fig. 5, compared to the full three-dimensional fundamental metallicity relation as given by Mannucci et al. (2010, their equation 2). In the L13 framework, galaxies evolve along the surface given by the fundamental metallicity relation.

Also, we wish to highlight the following point, which was not discussed in L13, but it is implied by the assumed $Z = f(\mathrm{sSFR})$ relation at a fixed epoch. It is in fact relevant to the data–model comparison to note that the galaxies in the $z = 2$ and 3

observational samples show a rather flat SFR–mass relation (cf. Mannucci et al. 2009, their fig. 6) by virtue of their selection. This relation is flatter than the typical SFR–mass relation for star-forming galaxies at the same epoch (e.g. Daddi et al. 2007). If we assume that the observational samples are culled out from the star-forming population at their respective redshifts, the selection of the most massive galaxies with systematically below the average SFR creates a bias such that the most massive galaxies tend to systematically have the lowest sSFR, and thus to be the most metal rich at their mass scale (at least this is the expectation in the L13 theoretical framework). By virtue of the SFR selection threshold, the low-mass galaxies will have higher than average SFR, and hence a lower metallicity than the typical star-forming galaxy at the same redshift and mass. This means that the observational samples might be biased in the direction of having a steeper mass–metallicity relation than the typical relation of an unbiased sample of star-forming galaxies at the same redshift. Therefore, any empirical conclusion on the evolution in the slope of the mass–metallicity relation must be treated with caution.

5.1.2 *On the L13 metallicity formula: accuracy and comparison to full numerical chemical evolution models*

In order to quantify the accuracy of the L13 approximations, we compared them to a full and direct numerical integration of the same equations, finding an excellent agreement (<0.1 dex) for three orders of magnitude in the sSFR and almost 2 dex in Z.

By comparing tracks in the $Z-$sSFR plane given by either the L13 approximation or the closed box relation to the predictions of full numerical chemical evolution models which relax some of the simplifying assumptions adopted in the analytic case, we find that in star-forming $z < 2$ (spiral) galaxies, where the sSFR slowly decreases with time, the system evolves along the locus of the steady-state solutions of decreasing gas fraction and increasing metallicity, exactly as in the L13 gas-regulated model. In particular, these systems seek the steady state metallicity without attaining it and the current metallicity is set by the current value of the sSFR.

Fast-forming (elliptical) galaxies evolve at higher sSFR than slowly evolving systems at the same metallicity, with a remarkable similarity to the well-known behaviour in the $[\alpha/\mathrm{Fe}] - [\mathrm{Fe/H}]$ plane. Their track in the sSFR–Z plane is better approximated by closed box models.

5.1.3 *The SFR as the second parameter in L13 and other special cases (closed box, evolution at constant gas mass)*

The actual functional form of a mass–(s)SFR–metallicity relation is quite controversial, with empirical findings also including claims of a reversal (namely high SFR would correspond to high metallicity) at high stellar masses (e.g. Yates et al. 2012) and a lack of any SFR effects at all masses (e.g. Sanchez et al. 2013). Clearly, differences may originate from a variety of empirical issues related to the sample specifics (including redshift range and aperture effects; e.g. Sanchez et al. 2013) as well as to the methods used to derive the metallicity (and the SFR).

In L13, the metallicity depends inversely on the sSFR. To some extent, we expect a smaller dependence on the sSFR as a second parameter at high masses, simply because in L13 ν becomes larger and hence the term sSFR/ν smaller than the other terms in the denominator of equation (8). In other words, the most massive models settle earlier on an evolutionary track where the metallicity quickly asymptotes to the yield, and the second parameter effect caused by variations in the (s)SFR becomes consequently small. It seems more difficult to explain a reversal of the trend above a given stellar mass scale.

Moreover, L13 model is meant to reproduce the average galaxy; therefore, it does not take into account that episodic bursts and mergers may also happen and move galaxies further out of the 'average' quasi-steady-state evolution represented by our tracks.

As a matter of fact, in this paper, we also show that an anticorrelation between Z and sSFR is found also in the early evolutionary phases of the closed box model.

In other works (e.g. Davé et al. 2012), the case $\Lambda - \eta = 1$ (which is a generalization of the Larson 1972 *extreme infall* in the context of analytic chemical evolution) has been dubbed 'steady-state'. In other words, all the net accreted gas is used up to form stars. More specifically, it is the $\Lambda = 1$, $\eta = 0$ case which is known as the 'extreme infall'. It has the property of preserving the gas mass, rather than the gas fraction, and that the metallicity would evolve as $Z = (Z_A + y_z)\,(1 - \exp(1/\mu - 1))$, asymptotically approaching the yield for μ approaching 0.

The generalization of *extreme infall* where both inflows and outflows are present (Λ, $\eta =$ const) has the following analytical solution for the metallicity:

$$Z = \frac{(Z_A \Lambda + y_z)}{\Lambda} \left\{1 - \mathrm{e}^{-\Lambda\,(1/\mu - 1)}\right\} \tag{32}$$

or equivalently

$$Z = \frac{[Z_A(1+\eta) + y_z]}{(1+\eta)} \left\{1 - \mathrm{e}^{-(1+\eta)(1/\mu - 1)}\right\}. \tag{33}$$

It is important to note here that, despite assuming the validity of the condition $\Lambda - \eta \simeq 1$, Davé et al. (2012) do not fully derive these solutions. In fact, they base their model on their equation (9). We find that their formula can be re-arranged, after discarding the trivial solution $Z(t) = 0$ and assuming that $Z \neq Z_A$, as $Z \sim \frac{[Z_A(1+\eta)+y_z]}{(1+\eta)}$, which is only an approximation to our exact solutions (e.g. equation 33), valid when the gas fraction is small (as pointed out also by Dayal et al. 2013). This latter condition ($\mu \ll 1$) is unlikely to be true in high-redshift galaxies.

When the galaxy is in its asymptotic regime at constant gas mass, that is, $Z \simeq Z_A + y_z$, the only way to increase its metallicity is by acting on $Z_A \neq 0$. In the first place, in the light of our full analytic derivation, we stress that the correct solutions for Z in a standard analytic chemical evolution model, when the infalling gas metallicity changes with time and it is linked to the past history of the galaxy, must take into account that $Z_A = Z_A(t)$ in the formal integration (equation 22 in this paper, see also the implementation of galactic fountains in Recchi et al. 2008).

We then note that when Z_A drives the metallicity, it increases with time in a manner that is not necessarily linked to the sSFR evolution. In other words, in systems with $\Lambda(-\eta) \sim 1$, the gas fraction still changes with time, leading to changes in the sSFR which are uncorrelated to variations in the gas metallicity (in principle, set by yield, and varied through a changing metallicity in the 're-accretion' of previously ejected material). This also implies that the scatter around the average $Z-$sSFR relation cannot be described by the same equation that governs the $Z = Z(\mathrm{sSFR})$ evolution as in L13. On the contrary, in Davé et al. (2012), the explanation of the scatter (and of the $Z-$sSFR anticorrelation) requires stochastic events that drive the galaxies out of equilibrium, either enhancing the SFR (e.g. mergers) or momentarily suppressing it (e.g. a sudden decrease in the accretion), and causing either a decrease or an increase in Z, respectively. This perspective is not dissimilar to the ex-

planation given by Mannucci et al. (2010) when they first presented the empirical results on the 'fundamental metallicity relation', and it is further extended in other recent work (e.g. Forbes et al. 2013) which depict both the mass–SFR and the mass–Z relations as the result of statistical equilibrium in the galaxy population at a given epoch.

5.2 Stellar metallicities in the L13 model

As a further extension of the L13 model, we show that it also naturally predicts a mass–metallicity relation in the stellar component which matches the current data at different epochs.

We compare our predictions to the data, and despite the encouraging qualitative agreement, no firm quantitative conclusions can be drawn due to: (i) the large scatter in the high-redshift data; (ii) the lack of consistency among the stellar metallicity measurements at different epochs and (iii) the presence of both passive and star-forming galaxies in the $z \sim 0$ data set.

L13's slowly evolving galaxies therefore match both the observed cosmic evolution in the gas and in the average stellar metallicity at a given mass. This is a consequence of the fact that the average stellar metallicity systematically lags ∼0.1–0.2 behind the gas metallicity of the same galaxy (as observed).

In evolved ($\mu \ll 1$) systems, such a small difference can be explained by the fact that both the gas and the average stellar metallicity tend to the yield. Whereas, during earlier stages of the evolution, the explanation lies in the fact that the SFR is steadily increasing in time. Therefore, the youngest stellar generations (whose composition is the same of the gas-phase) have a larger weight in the computation of the average stellar metallicity.

These findings imply that the evolution of the average stellar metallicity in the early phases of L13 galaxies as a function of the sSFR can be approximated by the same formula adopted for the gas phase metallicity.

ACKNOWLEDGEMENTS

We thank the referee for the comments that improved the quality of the paper.

REFERENCES

Arimoto N., Yoshii Y., 1987, A&A, 173, 23
Belli S., Jones T., Ellis R. S., Richard J., 2013, ApJ, 772, 141
Bordoloi R. et al., 2011, ApJ, 743, 10
Bordoloi R. et al., 2013, ApJ, preprint (arXiv:1307.6553B)
Bouché N. et al., 2010, ApJ, 718, 1001
Calura F., Pipino A., Chiappini C., Matteucci F., Maiolino R., 2009, A&A, 504, 373
Christensen L. et al., 2012, MNRAS, 427, 1953
Cid Fernandes R., Asari N. V., Sodré L., Stasińska G., Mateus A., Torres-Papaqui J. P., Schoenell W., 2007, MNRAS, 375, L16
Clayton D. D., 1988, MNRAS, 234, 1
Cresci G., Mannucci F., Sommariva V., Maiolino R., Marconi A., Brusa M., 2012, MNRAS, 421, 262
Cullen F., Cirasuolo M., McLure R. J., Dunlop J. S., 2014, MNRAS, 440, 2300
Daddi E. et al., 2007, ApJ, 670, 156
Dalcanton J. J., 2007, ApJ, 658, 941
Davé R., Finlator K., Oppenheimer B. D., 2012, MNRAS, 421, 98
Dayal P., Ferrara A., Dunlop J. S., 2013, MNRAS, 430, 2891
Dutton A. A., van den Bosch F. C., Dekel A., 2010, MNRAS, 405, 1690
Edmunds M. G., 1990, MNRAS, 246, 678
Elbaz D. et al., 2007, A&A, 468, 33
Ellison S. L., Patton D. R., Simard L., McConnachie A. W., 2008, ApJ, 672, L107
Erb D. K., Shapley A. E., Pettini M., Steidel C. C., Reddy N. A., Adelberger K. L., 2006a, ApJ, 644, 813
Erb D. K., Steidel C. C., Shapley A. E., Pettini M., Reddy N. A., Adelberger K. L., 2006b, ApJ, 646, 107
Forbes J. C., Krumholz M. R., Burkert A., Dekel A., 2013, preprint (arXiv:1311.1509)
Gallazzi A., Charlot S., Brinchmann J., White S. D. M., 2006, MNRAS, 370, 1106
Garnett D. R., 2002, ApJ, 581, 1019
González V., Labbé I., Bouwens R. J., Illingworth G., Franx M., Kriek M., Brammer G. B., 2010, ApJ, 713, 115
Halliday C. et al., 2008, A&A, 479, 417
Hartwick F. D. A., 1976, ApJ, 209, 418
Henry A. et al., 2013, ApJ, 776, L27
Köppen J., Edmunds M. G., 1999, MNRAS, 306, 317
Köppen J., Weidner C., Kroupa P., 2007, MNRAS, 375, 673
Krumholz M. R., Dekel A., McKee C. F., 2012, ApJ, 745, 69
Lara-López M. A. et al., 2010, A&A, 521, L53
Lara-López M. A. et al., 2013, MNRAS, 434, 451
Larson R. B., 1972, Nature, 236, 21
Leja J. et al., 2013, ApJ, 778, L24
Lequeux J., Peimbert M., Rayo J. F., Serrano A., Torres-Peimbert S., 1979, A&A, 80, 155
Lilly S. J., Carollo C. M., Pipino A., Renzini A., Peng Y., 2013, ApJ, 772, 19 (L13)
Maier C., Lilly S. J., Carollo C. M., Stockton A., Brodwin M., 2005, ApJ, 634, 849
Maier C., Lilly S. J., Carollo C. M., Meisenheimer K., Hippelein H., Stockton A., 2006, ApJ, 639, 858
Maiolino R. et al., 2008, A&A, 488, 463
Mannucci F. et al., 2009, MNRAS, 398, 1915
Mannucci F., Cresci G., Maiolino R., Marconi A., Gnerucci A., 2010, MNRAS, 408, 2115
Mannucci F., Salvaterra R., Campisi M. A., 2011, MNRAS, 414, 1263
Matteucci F., 1994, A&A, 288, 57
Matteucci F., 2001, in Matteucci F., ed., Astrophysics and Space Science Library, Vol. 253, The Chemical Evolution of the Galaxy. Kluwer, Dordrecht, p. 293
Matteucci F., Brocato E., 1990, ApJ, 365, 539
Matteucci F., Chiosi C., 1983, A&A, 123, 121
Moster B. P., Somerville R. S., Maulbetsch C., van den Bosch F. C., Macciò A. V., Naab T., Oser L., 2010, ApJ, 710, 903
Nakajima K., Ouchi M., 2013, preprint (arXiv:1309.0207)
Newman S. F. et al., 2012, ApJ, 761, 43
Niino Y., 2012, ApJ, 761, 126
Noeske K. G. et al., 2007, ApJ, 660, L43
O'Connell R. W., 1976, ApJ, 206, 370
Oliver S. et al., 2010, MNRAS, 405, 2279
Pagel B. E. J., Patchett B. E., 1975, MNRAS, 172, 13
Pannella M. et al., 2009, ApJ, 698, L116
Panter B., Jimenez R., Heavens A. F., Charlot S., 2008, MNRAS, 391, 1117
Peeples M. S., Shankar F., 2011, MNRAS, 417, 2962
Peng Y.-J. et al., 2010, ApJ, 721, 193
Pipino A., Matteucci F., 2004, MNRAS, 347, 968
Pipino A., Matteucci F., Chiappini C., 2006, ApJ, 638, 739
Pipino A., Devriendt J. E. G., Thomas D., Silk J., Kaviraj S., 2009, A&A, 505, 1075
Pipino A., Fan X. L., Matteucci F., Calura F., Silva L., Granato G., Maiolino R., 2011, A&A, 525, 61
Pipino A., Calura F., Matteucci F., 2013, MNRAS, 432, 2541
Recchi S., Spitoni E., Matteucci F., Lanfranchi G. A., 2008, A&A, 489, 555
Reddy N. A., Steidel C. C., Fadda D., Yan L., Pettini M., Shapley A. E., Erb D. K., Adelberger K. L., 2006, ApJ, 644, 792
Richard J., Jones T., Ellis R., Stark D. P., Livermore R., Swinbank M., 2011, MNRAS, 413, 643

Rix S. A., Pettini M., Leitherer C., Bresolin F., Kudritzki R.-P., Steidel C. C., 2004, ApJ, 615, 98
Rosales-Ortega F. F., Sánchez S. F., Iglesias-Páramo J., Díaz A. I., Vílchez J. M., Bland-Hawthorn J., Husemann B., Mast D., 2012, ApJ, 756, L31
Sakstein J., Pipino A., Devriendt J. E. G., Maiolino R., 2011, MNRAS, 410, 2203
Sanchez S. F. et al., 2013, A&A, 554, 58
Savaglio S. et al., 2005, ApJ, 635, 260
Schmidt M., 1959, ApJ, 129, 243
Schmidt M., 1963, ApJ, 137, 758
Sommariva V., Mannucci F., Cresci G., Maiolino R., Marconi A., Nagao T., Baroni A., Grazian A., 2012, A&A, 539, 136
Spitoni E., Calura F., Matteucci F., Recchi S., 2010, A&A, 514, 73
Stark D. P., Schenker M. A., Ellis R., Robertson B., McLure R., Dunlop J., 2013, ApJ, 763, 129
Stott J. P. et al., 2013, MNRAS, 436, 1130
Tinsley B. M., 1980, Fundam. Cosm. Phys., 5, 287
Tremonti C. A. et al., 2004, ApJ, 613, 898
Troncoso P. et al., 2014, A&A, 563, A58
Twarog B. A., 1980, ApJ, 242, 242
Weiner B. J. et al., 2005, ApJ, 620, 595
Wuyts E., Rigby J. R., Sharon K., Gladders M. D., 2012, ApJ, 755, 73
Yates R. M., Kauffmann G., Guo Q., 2012, MNRAS, 422, 215
Yuan T.-T., Kewley L. J., Richard J., 2013, ApJ, 763, 9
Zahid H. J., Bresolin F., Kewley L. J., Coil A. L., Davé R., 2012, ApJ, 750, 120
Zahid H. J. et al., 2013, preprint (arXiv:1310.4950)

APPENDIX A

The impact of the assumed star formation law

Let us discuss the impact of a more general star formation law on our results, that, for the purpose of this discussion, we write as $\psi = \nu M_{\rm gas}^{(1+x)}$. In this paper, we presented the results for the case $x = 0$. Such a linear Schmidt volumetric relation is a standard assumption in the literature and it has the advantage of a slight simplification of the calculations presented in this paper. To corroborate our assumption, we note that in a recent paper, Krumholz et al. (2012) showed that a simple volumetric star formation law as the one adopted in our paper can explain a wide range of both local and high-redshift observations.

Furthermore, it leads us to a relation with exponent 1.5 if the star formation efficiency is expressed in units of the local free fall time, and this latter quantity is in turn expressed as a function of the gas volume density. This also ensures compatibility with the expression adopted in studies where SFR and density are in units of surface which assume an exponent $x \sim 1.4$.

It is well known that the solutions of the form $Z = Z(\mu)$ of analytical chemical evolution models do not explicitly depend on the SFR (and its law). Therefore, the particular star formation law adopted does not influence these general results. It is the conversion of the gas fraction into sSFR that introduces a dependence on the assumed star formation law in the equations of the form $Z = Z(\mathrm{sSFR})$. To see the impact of the change let us proceed as in the main body of the paper, namely let us focus on the steady-state solutions and the derive more general statements.

In the case of the steady state, the results presented in equations (12)– (14) and (16) (its first row), as well as other results like equations (32) and (33), will not depend on x as they do not feature any explicit dependence on the star formation law.

On the other hand, when $x \neq 0$, equation (1) would be

$$\mathrm{sSFR}/\nu \propto \frac{\mu}{1+\mu}\mu^x$$

(e.g. Reddy et al. 2006, when $x = 0.4$) and equation (15) would read as

$$\mathrm{sSFR}/\nu = (\Lambda - \eta - 1)M_{\rm gas}^x\,.$$

The steady state solution presented in Section 3.2 (equation 16, second row) will then be

$$Z = \frac{1}{1+\eta+\mathrm{sSFR}/(\nu M_{\rm gas}^x)}\,,$$

where for simplicity we ignore the metallicity of the infalling gas. If $x > 0$, the system behaves as if it has a higher effective star formation efficiency $\nu M_{\rm gas}^x$. Moreover, $x \neq 0$ would imply an evolution at constant gas fraction and metallicity with the sSFR still changing in time as $M_{\rm gas}^x$.

Given the close link between I_1 (equation 11), equation (24) and the steady-state solution (equation 16), we expect a similar variation, namely the appearance of a factor $\sim M_{\rm gas}^x$ in the expression for $Z_{\rm L13}$ in both the ideal and non-ideal case, as well as in the general solutions. More quantitatively, this happens because the term G in the differential equation (19) will now be

$$G(\mathrm{sSFR}) = \frac{1+\frac{Z_A\Lambda}{y_z}}{\mathrm{sSFR}/\nu((1+x)(\Lambda-\eta-1)M_{\rm gas}^x - \mathrm{sSFR}/\nu)}\,, \quad \text{(A1)}$$

leading to a change in the expression for $F(\mathrm{sSFR})$ too. The qualitative description of the galaxy behaviour will not change: as these models tend to a $\Lambda \sim 1$ (constant gas mass) evolution in the long term, the factor $M_{\rm gas}^x$ will be merely a constant for all practical purposes.

This paper has been typeset from a TEX/LATEX file prepared by the author.